Accepted Manuscript

Temperature dependent thermal conductivity of magnetocaloric materials: impact assessment on the performance of active magnetic regenerative refrigerators

D.J. Silva, A. Davarpanah, J.S. Amaral, V.S. Amaral

PII: S0140-7007(19)30267-1
DOI: https://doi.org/10.1016/j.ijrefrig.2019.06.016
Reference: JIJR 4436

To appear in: *International Journal of Refrigeration*

Received date: 2 April 2019
Revised date: 24 May 2019
Accepted date: 11 June 2019

Please cite this article as: D.J. Silva, A. Davarpanah, J.S. Amaral, V.S. Amaral, Temperature dependent thermal conductivity of magnetocaloric materials: impact assessment on the performance of active magnetic regenerative refrigerators, *International Journal of Refrigeration* (2019), doi: https://doi.org/10.1016/j.ijrefrig.2019.06.016

Highlights

- Magnetocaloric systems are evaluated for refrigerant T-dependent conductivities.
- The temperature span and power is affected 15 % for changes of conductivity of 50
- The impact on longitudinal and axial thermal conduction is discussed.

Temperature dependent thermal conductivity of magnetocaloric materials: impact assessment on the performance of active magnetic regenerative refrigerators

D. J. Silva[a,1], A. Davarpanah[a], J. S. Amaral[a], V. S. Amaral[a]

[a]*Department of Physics and CICECO - Aveiro Institute of Materials, University of Aveiro, 3810-193 Aveiro, Portugal*

Abstract

Due to the dynamic nature of the active magnetic regenerative mechanism in magnetocaloric refrigeration, the thermal conductivity of the refrigerant is a critical parameter. Experimental studies have shown how the thermal conductivity of high-performance magnetic refrigerants can drastically change around their Curie temperatures (T_C). However, this fact has been largely ignored in the numerical simulation of devices, raising the need to assess the impact of this approximation, particularly when the simulations are aimed at optimizing or dimensioning a particular device geometry. In this paper we show how, by employing a unidimensional numerical model of a magnetic refrigerator with parallel plates, two different temperature dependent thermal conductivity scenarios of the refrigerant affect the resulting temperature span and cooling power. By considering a gadolinium-like material as the refrigerant with thermal conductivities varying 50% near its T_C, a change of the resulting device temperature span of $\sim 15\%$ is reached. The cooling

Email address: djsilva@ua.pt (D. J. Silva)

power is also affected, changing also $\sim 15\%$ when the considered systems are at half their respective maximum temperature span. Our results are also discussed in terms of other geometries where the impact of these effects can be even larger, namely in cases where the axial thermal conduction in the AMR element is not negligible, or the time-scale of longitudinal thermal processes has a larger impact on the optimum operating frequency.

Keywords: Magnetic refrigeration, Active magnetic regeneration, Magnetocaloric effect

1. Introduction

Magnetocaloric refrigeration has been pointed out as one of the most reliable alternatives to vapor compression-based systems since it has a high efficiency and does not need to use nocive gases [1]. It relies on the magnetocaloric effect where magnetization and demagnetization of magnetocaloric materials is followed by a change of entropy [2]. Today, the most commonly used magnetocaloric refrigeration mechanism relies on the active magnetic regenerative (AMR) cycle, which can be seen as a cascade of Brayton cycles (two adiabatic and two isofield processes). In the AMR cycle, a magnetic field (H) is applied to a porous magnetocaloric material followed by the flow of a fluid in the material in one direction. In the second stage, H is removed and the fluid flows in the opposite direction [2–5]. Since the magnetocaloric material (MCM) is used as both the refrigerant and heat reservoir, it behaves as a regenerator in a dynamic process [6].

One way to maximize the heat transfer process between the fluid and the

Nomenclature

Greek	
Δ	Difference
ν	frequency (Hz)
ρ	density (kgm^{-3})
τ	period of the fluid flow (s)
Superscript	
n	time index
Roman	
C	specific heat ($Jkg^{-1}K^{-1}$)
$CHEX$	Cold heat exchanger
COP	coefficient of performance
H	magnetic field (Am^{-1})
HEX	Heat exchanger
$HHEX$	Hot heat exchanger
k	thermal conductivity ($Wm^{-1}K^{-1}$)
l	regenerator length unit (m)
MCM	Magnetocaloric material
p	heat transfer power per volume (Wm^{-3})
s	stroke (cm)
T	temperature (K)
t	time (s)
v	velocity (ms^{-1})
x	position (m)
A	cross-sectional area (m^2)
a	specific surface
D	Diameter(m)
m	mass (Kg)
Nu	Nusselt number
Subscript	
ad	adiabatic
f	fluid
H	at constant magnetic field
i	space index
max	maximum
s	solid
C	Curie
Gd	Gadolinium
h	hydraulic
r	ratio

MCM is by optimizing the utilization factor defined by [2]:

$$U = \frac{\dot{m}_f C_{H,f} \tau}{m_{\mathrm{MCM}} \langle C_{p,\mathrm{MCM}} \rangle}, \tag{1}$$

where $\dot{m}_f$ is the mass flow rate of the fluid, $C_{H,f}$ is the heat capacity of the fluid, τ is the period of the fluid flow, m_{MCM} is the mass of the MCM, and $\langle C_{p,\mathrm{MCM}} \rangle$ is the average of the heat capacity of the MCM. A large utilization factor increases the heat transfer processes in such a way that the regenerative effect vanishes. On the other hand a small utilization factor reduces the heat transfer processes between the fluid and the MCM, which decreases the regenerative effect as well, and, therefore, reduces the final temperature span.

Since the AMR process is dynamic, it strongly depends on the thermal conductivities (k), in particular that of the MCM. This fact makes the utilization factor only applicable for certain systems where the heat conduction on directions perpendicular to the fluid flow (longitudinal direction) is a very fast process [7]. By considering Δl as the maximum solid distance in the perpendicular direction to the fluid flow within the MCM, one can deduce that the utilization factor can only be applied if

$$\Delta l < \sqrt{\frac{k\tau}{C_H \rho'}}, \tag{2}$$

where ρ' is the unidimensional density of the MCM. Equation 2 is applied for the majority of the regenerator geometries. In particular, the thickness of parallel plates and the diameter of packed spheres are, in general, small. On the contrary, the dynamic AMR process strongly depends on the axial heat conduction since the time constant of the heat transfer processes are typically large due to the length of the regenerator: on one hand the fluid transfers

heat from one section of the magnetocaloric material to another section; on the other hand heat is conducted axially within the magnetocaloric material. Therefore, the goal of the regenerative process is to reduce as much as possible axial conduction but still have heat transfer processes between the fluid and the magnetocaloric material.

One important aspect of the thermal conductivity (k) of magnetocaloric materials is its dependence with temperature. In that respect, several investigations have been reporting considerable variations. M. B. Salamon and M. Jaime compiled data of manganites concerning their transport properties for several structures, in particular $LaCaMnO_3$ can change k one order of magnitute in the range 200-300 K [8]. Fujieda et al. reported data for the thermal conductivities of LaFeSi and GdSiGe compound families, where in some cases it was shown a change of $\sim 100\%$ within the range 200-300 K [9, 10]. Luybina et al. developed a novel bulk $La(Fe, Si)_{13}/Cu$ composite that showed a significant k in the same range window of 200-300 K [11]. Gamzatov et al. measured the thermal conductivity of $Pr_{0.6}Sr_{0.4}Mn_{1-x}Fe_xO_3$ manganites, again with a change in thermal conductivity near 100% between 200 and 300 K [12]. More recently, Wada et al. studied the temperature dependence of k of $Mn_{1.03}As_{0.70}Sb_{0.30}$ and Ru-doped or Ni-doped $(MnFeRu)_2(PSi)$. The authors reported the duplication of k in the temperature window of 200-300 K [13]. In summary, near room temperature several magnetocaloric materials change considerably their thermal conductivities.

Incorporating correct values of k into physical models is of paramount importance. However, only fixed values of k has been considered in modeling magnetocaloric system [14–20]. In this work we performed a systematic

numerical investigation on the implications of using different types of $k(T)$ curves with temperature on the performance of active magnetic regenerative systems (temperature span and cooling power). We show that using different curves of $k(T)$ in a gadolinium MCM leads to a change of the temperature span and cooling power of an active magnetic refrigerator with a parallel plates regenerator.

2. Model

The python heatrapy package was used to compute the active magnetic refrigerator [21]. The modeled system is unidimensional and is described in Ref. [22] for hydraulic active magnetic regenerative systems. As depicted in Fig. 1, it consists of four unidimensional elements: one fluid, one MCM plate, one hot reservoir (HR), also known as hot heat exchanger (HHEX), and one cold reservoir (CR), also known as cold heat exchanger (CHEX). The heat transfer processes taking place between them takes into account the geometry of the plates. This concept has been used in several numerical investigations [15] and are, in principle, enough for describing the overall process of the active magnetic regenerative effect. The governing equations are the following [23]:

$$\rho_s C_{H,s} \frac{\partial T_s}{\partial t} - \frac{\partial}{\partial x}\left(k_s \frac{\partial T_s}{\partial x}\right) + p_s = 0, \tag{3}$$

$$\rho_f C_{H,f} \left(\frac{\partial T_f}{\partial t} + v\frac{\partial T_f}{\partial x}\right) - \frac{\partial}{\partial x}\left(k_f \frac{\partial T_f}{\partial x}\right) + p_f = 0, \tag{4}$$

where T is the temperature, x the space coordinate, t the time, ρ the density of the material, C_H the specific heat at constant H, k the thermal conductivity, v the velocity of the fluid, p the heat transfer power per volumne

material	C_p J/(KgK)	k W/(mK)	ρ Kg/m^3	ΔT_{ad}^{+} (K)	ΔT_{ad}^{-} (K)
water	4200	0.6	1000	0	0
Gd	t.d.	t.d.	7900	t.d.	t.d.
Cu	385	401	8933	0	0

Table 1: Physical properties of the used materials in the modeled system. t.d. stands for temperature-dependent.

between the solids and fluid, and the subscript s and f defines the type of material, solid or fluid, respectively. In the present model one considers the fluid framework so that the fluid is static ($v = 0$) and the other three components are moving forward and backward as shown in Fig. 1. In this context, the convective term of Eq. 4 vanishes and the overall problem is reduced to a heat conduction problem. The equations were solved by using the Crank-Nicholsen implicit finit difference method with the `'implicit_k(x)'` solver of the heatrapy package [22]:

$$\begin{aligned} &-(k_{i-1}^{n+1} + k_i^{n+1})T_{i-1}^{n+1} + \\ &(\gamma_i + k_{i+1}^{n+1} + 2k_{i-1}^{n+1})T_i^{n+1} - \\ &(k_{i+1}^{n+1} + k_i^{n+1}) = \\ &= (k_{i-1}^{n+1} + k_i^{n+1})T_{i-1}^{n} + \\ &(\gamma_i - k_{i+1}^{n+1} - 2k_i^{n+1} - k_{i-1}^{n+1})T_i^{n} + \\ &+ (k_{i+1}^{n+1} + k_i^{n+1})T_{i+1}^{n} + 4\Delta x^2 p_i^{n+1}, \end{aligned} \tag{5}$$

where i and n stands for the space and time index, Δx and Δt stands for the space and time steps respectively and $\gamma = \frac{4\rho_i^{n+1} C_i^{n+1} \Delta x^2}{\Delta t}$.

The heat transfer coefficients depend on the type of regenerator. Since

the parallel plates regenerator is considered for the present model the heat transfer between the solid and fluid is given by

$$p_f = \frac{\mathrm{Nu} k_f a_s A}{D_h}(T_f - T_s), \tag{6}$$

where Nu is the Nusselt number, that is approximately 7.541 for a set of parallel plates [6, 24], and a_s, D_h, and A are the specific surface, the hydraulic diameter, and the cross-sectional area, respectively. The heat transfer power per length between the solids and fluid used by the MCM, CR and HR is $p_s = -p_f$. The hydraulic diameter and specific surface are given by

$$D_h = 2l_f, \tag{7}$$

$$a_s = \frac{2}{l_s + l_f}, \tag{8}$$

where l_s and l_f are the regenerator plate height and fluid channel height, respectively. The magnetocaloric effect was considered by shifting the temperature between time instants [22]:

$$T_i^{n+1} = T_i^n \pm \Delta T_{ad}^{\pm}(T_i^n), \tag{9}$$

where - and + stands for the removal and application of H, so that ΔT_{ad}^{+} and ΔT_{ad}^{-} accounts for the adiabatic temperature change when applying and removing H, respectively.

To obtain temperature span values insulation was imposed for CR, and HR was kept at a fixed operating temperature [25–27]. On the other hand, to obtain cooling power quantities the temperature of both reservoirs were kept at fixed values. The fixed temperature boundary conditions are considered by keeping constant the temperature of the boundary point:

$$T_b^{n+1} = T_b^n, \tag{10}$$

where b is the boundary space index. Thermal insulation is modeled by keeping the temperature of the previous point equal of the boundary point:

$$T^n_{b\pm1} = T^n_b. \tag{11}$$

To investigate how the curve of thermal conductivities influences the performance of an active magnetic refrigerator three curves were used as shown in Fig. 2: one curve with constant k (equal to the thermal conductivity of Gd at 293 K, 10 W/(mK)), one curve with increasing k with temperature (Gd+), and one curve with decreasing k with temperature, obeying the following equations:

$$k_{Gd-} = \begin{cases} k_{min}, & \text{if T} < T_C \\ \sqrt{\Delta k^2 - (T - T_C + \Delta k)} + k_{min}, & \text{if T} > T_C \end{cases} \tag{12}$$

$$k_{Gd+} = \begin{cases} \sqrt{\Delta k^2 - (T - T_C - \Delta k)} + k_{min}, & \text{if T} < T_C \\ k_{min}, & \text{if T} > T_C \end{cases} \tag{13}$$

where k_{min} = 8.4 K, T_C=293 K, and Δk = 4.2 W/(mK). While k of Gd- decreases 50 %, the k curve of Gd+ increases 50%, relative to k_{min}. A change of 100%, reported by many investigations as described in the introduction section, was not the choice of the present investigation since the temperature window of magnetocaloric systems are more reduced (typically up to $\sim$ 20 K).

The used value for C_H and ρ for Gd were extracted from Ref. [17] (Fig. 3). While C_H is strongly dependent on temperature, ρ can be considered as being fixed at 7900 Kg/m^3. Water was chosen for the fluid. Note that for dimensioning actual systems one must consider thermal properties of heat

exchangers. For the simplicity of the current model, and to focus on the purpose of the present investigation, we have used the thermal properties of copper for both reservoirs. All the physical properties of the used materials in the modeled system is listed in table 1. Finally, the used space and time steps were 0.1 cm and 0.005 s, respectively. The length of the fluid, MCM, HR and CR were 16 cm, 5 cm, 2 cm and 2 cm, respectively. The modeled stroke that dictates the motion of the fluid was 2.5 cm, i.e. in the present case the motion amplitude of the reservoirs and MCM was 2.5 cm. This value allowed to incorporate a non-negligible regenerative effect. The considered thickness of each parallel plate was 1 mm, and the spacing between them was 1 mm. These values can vary in some magnetocaloric prototypes described in literature [2], although within the same order of magnitude considered in the present investigation.

Finally, one should analyze the validity of the unidimensional model to the considered AMR system. Petersen et al. compared 1D and 2D numerical models for active magnetic regenerative refrigerators and concluded that 1D models are sufficient to describe the related behavior if temperature gradients in the perpendicular direction of the fluid flow is small [24]. This condition can only be met if the longitudinal heat transfer processes are fast enough, which can occur if Eq. 2 is verified. In the particular case of the present system Δl must be < 2.5 mm, which is verified since the thickness of each parallel plate is 1 mm.

3. Model validation and computation

For the temperature span investigation, both the frequency and the operating temperature were sweeped. Therefore, a total of 3×17×30=1530 simulations were carried out (3 Gd investigations, 17 frequencies and 30 operating temperatures). For the cooling power investigation the temperature span was kept constant at 10 different values, ranging from 0 to 100% of the maximum temperature span (no load temperature span). This was done for the operating temperatures 298 K, 302 K and 305 K. In this case the operating frequency was kept constant at 0.07 Hz. For the computation a workstation with 28 physical cores Intel(R) Xeon(R) CPU E5-2690 v4 @ 2.60 GHz were used.

To validate the present simulations 4 tests were performed: (i) First, a comparison of the used refrigeration system model with Gd for the MCM was made with the numerical work of Petersen et al. [17]. For the frequency of 0.167 Hz, a temperature span of 11.61 K was obtained with our model, compared to 10.9 K of ref. [17] (error of $\sim$ 3.5 %). (ii) Another performed validation was the verification of invariant temperature span when changing the first magnetocaloric effect step. Applying H or removing H in the first cycle of the operation led to the same results since the hot reservoir (HHEX) is at a fixed temperature and the cold reservoir (CHEX) is insulated. (iii) At the maximum temperature span, the cooling power must be 0, which was verified in the cooling power study for all the considered three operating temperatures, as observed in Fig. 6. (iv) Finally, at zero cooling power the temperature span must be maximum (ΔT_{max}), which was also verified in the cooling power study (see Fig. 6).

4. Results and discussion

From Fig. 4 (g), (h), and (i) one can observe that three different regimes occur for different operating temperatures. At 298 K, Gd+ has the largest no load temperature span (ΔT_{max}), followed by Gd. The smallest ΔT_{max} occurs for Gd-. At the operating temperature of 302 K ΔT_{max} is approximately the same for all the MCM model types. For the operating temperature of 305 K, ΔT_{max} is largest for Gd- and smallest for Gd+. Note that for large frequencies the difference between the three MCM models vanishes. This can be observed in all the plots of Fig. 4 (g-i). This behaviour occurs since for large frequencies the period is too small for the axial conduction to occur before switching the flow of the liquid, so that the axial conduction plays a minor role in the heat transfer. The difference of the temperature span for different MCM models when the frequencies tend to 0 also reduces. However, in this case this reduction is due to the fact that in the limit of 0 Hz all the curves must present the same value of 0 K.

Since Eq. 2 is verified for the present system, the role of the longitudinal heat conduction is negligible on the dynamic AMR process. Therefore, it is expected that the less the k (axial conduction) the largest the temperature span. In fact, from Figs. 4 (a-i) one can observe that the smaller the average k the largest temperature span. For example, for the operating temperature 298 K, Gd+ has an average k over the x-axis smaller than Gd and Gd-, making Gd- a better material for small operating temperatures. The opposite behavior occurs for large temperature spans, where the average k of Gd- is smaller than Gd and Gd+. For the operating temperature of 302 K, the average k is approximately the same for all the MCM models so that ΔT_{max}

is approximately the same.

Figure 5 shows the temperature span at 0.07 Hz as a function of operating temperature for the three MCM model types. It is clear that two different regimes occur: one at low operating temperatures ($<$ 302 K), and one at high operating temperatures ($>$ 302 K). The separation in two regimes is correlated with the average k of the MCM as pointed out in the last paragraph. Since the k of Gd+ increases with temperature, the smallest average k of the MCM in the stationary state occurs for small temperatures. On the contrary, since the k of Gd- decreases with temperature, the smallest average k in the stationary state occurs for large temperatures. The transition of the MCM model type for the temperature span happens at $\sim$ 302 K, which corresponds to the operating temperature where half of the MCM is at k_{min} and half at $k_{min} + \Delta k$ for both Gd- and Gd+. At this operating temperature, the average k of Gd- and Gd+ is approximately equal to the fixed k of Gd. Note that in Fig. 4 (h) at small frequencies the three curves diverge. This fact occurs since at this operating frequency the temperature span is smaller, and thus the change of k along the x-axis is no longer centered in the middle of the MCM, i.e. the difference of the average k for Gd- and Gd+ is no longer negligible.

The impact of using different MCM models on the performance of a magnetocaloric refrigerator is somewhat different when the key parameter is the cooling power. The main difference when compared to the temperature span is related to the operating temperature. Figure 6 shows the cooling power per area as a function of temperature span / maximum temperature span ratio (ΔT_r) for the three operating temperatures analyzed above (298K, 302

K and 305 K). First, one can observe that the cooling power per area tends to be the same for the three MCM models when approching ΔT_r to 0 and to 1. For $\Delta T_r = 0$ the temperature of the MCM is approximately uniform and, thus, the axial heat conduction has a minor role on the heat transfer processes. For $\Delta T_r = 1$, the system has attained ΔT_{max} and the cooling power per area has reached 0. From Fig. 6 it is clear that the maximum cooling power per area reduces with the operating temperature from 298 K to 305 K. Moreover, Gd+ shows always the smallest values. This trend comes from the fact that this difference among the three MCM model types occurs for $\Delta T_r \neq 1$. Thus, the average k of Gd+ is always larger for the 3 operating temperatures. Nevertheless, for smaller operating temperatures one expects that the cooling power of Gd+ becomes largest compared to Gd and to Gd-.

Finally, one must note that the optimum operating frequency was marginally changed for the three MCM model types. For instance, for the operating temperatures depicted in Fig. 4 only the optimum operating frequency was changed by a very small amount from Gd+ to Gd and to Gd- for the operating temperature 298 K. This occurs since the optimum operating frequency is mostly dictated by the geometry, the heat transfer processes between the MCM and fluid, the thermal properties of the fluid, and the longitudinal heat transfer processes of the MCM. Since one uses the same geometry and fluid in the present investigation, and since the heat transfer processes between the MCM and fluid can be considered the same when using Gd, Gd- and Gd+, only the longitudinal heat transfer processes can change when using different MCM model types. However, as already pointed out previously, the longitudinal heat processes for thin parallel plates are too fast and, therefore, they

do not limit the speed of the heat transfer processes of the overall system (Eq. 2 verified). Using different $k(T)$ curves can only influence significantly the operating frequency if using l values not satisfying 2, which is, in general, not the case for parallel plate and packed spheres regenerators.

5. Conclusions

We have performed a systematic numerical investigation on the influence of the temperature dependence of the thermal conductivity on the performance of active magnetic regenerative refrigeration systems using parallel plates MCMs as regenerator. We have used the heatrapy package to perform numerical simulations at 1.5D for regenerators based on parallel plates. Changes of thermal conductivities of $\sim 50\%$, compatible with observed experimental data, can lead to variations of temperature spans and cooling power quantities of $\sim 15\%$. $k(T)$ curves have impacts on the axial and longitudinal heat transfer processes within the magnetocaloric material. However, for most geometries, such as thin parallel plates regenerators, k values has typically a minor role in the longitudinal heat transfer processes if the thickness obey the condition $< \sqrt{\frac{k\tau_f}{C_H\rho'}}$. Therefore, in the present investigation these variations come from the fact that axial conduction plays an important role on the regenerative effect: the less axial conduction the better. Moreover, since the longitudinal thermal processes are too fast, the optimum operating frequency changed only marginally. Our results show clear evidence that neglecting the temperature dependence of the thermal conductivity of the magnetocaloric material affects the resulting performance of the magnetocaloric system.

Acknowledgement

The present study was developed in the scope of the Smart Green Homes Project [POCI-01-0247-FEDER-007678], a co-promotion between Bosch Termotecnologia S.A. and the University of Aveiro. It is financed by Portugal 2020 under the Competitiveness and Internationalization Operational Program, and by the European Regional Development Fund. Project CICECO-Aveiro Institute of Materials, POCI-01-0145-FEDER-007679 (FCT Ref. UID/CT/5001/2013), financed by national funds through the FCT/MEC and co-financed by FEDER under the PT2020 Partnership Agreement is acknowledged. JSA and AD acknowledge FCT IF/01089/2015 and SFRH/BD/103556/2014 research grants.

References

References

[1] K. Gschneidner Jr., V. Pecharsky, Thirty years of near room temperature magnetic cooling: Where we are today and future prospects, Int. J. Refrig. 31 (6) (2008) 945.

[2] A. Kitanovski, J. Tušek, U. Tomc, U. Plaznik, M. Ožbolt, A. Poredoš, Magnetocaloric Energy Conversion: From Theory to Applications, Springer, Springer Cham Heidelberg New York Dordrecht London, 1st edn., 2015.

[3] B. Yu, Q. Gao, B. Zhang, X. Meng, Z. Chen, Review on research of room trmperature magnetic refrigeration, Int. J. Refrig. 26 (6) (2003) 622.

[4] X. Moya, S. Kar-Narayan, N. D. Mathur, Caloric materials near ferroic phase transitions, Nat. Mater. 13 (5) (2014) 439.

[5] A. Kitanovski, U. Plaznik, U. Tomc, A. Poredoš, Present and future caloric refrigeration and heat-pump technologies, Int. J. Refrig. 57 (2015) 288.

[6] T. Lei, K. Engelbrecht, K. Nielsen, C. Veje, Study of geometries of active magnetic regenerators for room temperature magnetocaloric refrigeration, Applied Thermal Engineering 111 (2017) 1232–1243.

[7] K. K. Nielsen, K. Engelbrecht, The influence of the solid thermal conductivity on active magnetic regenerators, J. Phys. D: Appl. Phys. 45 (2012) 145001.

[8] M. Salamon, M. Jaime, The physics of manganites: Structure and transport, Reviews of Modern Physics 73 (3) (2001) 583–628.

[9] S. Fujieda, Y. Hasegawa, A. Fujita, K. Fukamichi, Thermal transport properties of magnetic refrigerants La(Fe xSi1-x)13 and their hydrides, and Gd 5Si2Ge2 and MnAs, Journal of Applied Physics 95 (5) (2004) 2429–2431.

[10] K. Fukamichi, A. Fujita, S. Fujieda, Large magnetocaloric effects and thermal transport properties of La(FeSi)13 and their hydrides, Journal of Alloys and Compounds 408-412 (2006) 307–312, doi: 10.1016/j.jallcom.2005.04.022.

[11] J. Lyubina, U. Hannemann, L. Cohen, M. Ryan, Novel la(fe,si) 13 /cu

composites for magnetic cooling, Advanced Energy Materials 2 (11) (2012) 1323–1327, doi:10.1002/aenm.201200297.

[12] A. Gamzatov, A. Batdalov, A. Aliev, Z. Khurshilova, M. Ellouze, F. Jemma, Specific heat, thermal diffusion, thermal conductivity and magnetocaloric effect in Pr0.6Sr0.4Mn1-xFexO3 manganites, Journal of Magnetism and Magnetic Materials 443 (2017) 352–357, doi: 10.1016/j.jmmm.2017.07.088.

[13] H. Wada, K. Fukuda, T. Ohnishi, K. Soejima, K. Otsubo, K. Yamashita, Thermal conductivity of giant magnetocaloric Mn compounds, Journal of Alloys and Compounds (2019) 445–451doi: 10.1016/j.jallcom.2019.01.188.

[14] K. Nielsen, C. Bahl, A. Smith, R. Bjørk, N. Pryds, J. Hattel, Detailed numerical modeling of a linear parallel-plate Active Magnetic Regenerator, International Journal of Refrigeration 32 (6) (2009) 1478–1486.

[15] K. Nielsen, J. Tusek, K. Engelbrecht, S. Schopfer, A. Kitanovski, C. Bahl, A. Smith, N. Pryds, A. Poredos, Review on numerical modeling of active magnetic regenerators for room temperature applications, International Journal of Refrigeration 34 (3) (2011) 603–616.

[16] C. Aprea, A. Maiorino, A flexible numerical model to study an active magnetic refrigerator for near room temperature applications, Applied Energy 87 (8) (2010) 2690–2698.

[17] T. F. Petersen, N. Pryds, A. Smith, J. Hattel, H. Schmidt, H. J. Høgaard Knudsen, Two-dimensional mathematical model of a recipro-

cating room-temperature Active Magnetic Regenerator, Int. J. Refrig. 31 (3) (2008) 432.

[18] T. Burdyny, A. Rowe, Simplified modeling of active magnetic regenerators, International Journal of Refrigeration 36 (3) (2013) 932–940.

[19] K. Engelbrecht, J. Tušek, K. Nielsen, A. Kitanovski, C. Bahl, A. Poredoš, Improved modelling of a parallel plate active magnetic regenerator, Journal of Physics D: Applied Physics 46 (25) (2013) 255002.

[20] S. Lionte, M. Risser, C. Vasile, L. Elouad, C. Muller, Adapting an active magnetic regenerator to a continuous fluid flow application, International Journal of Refrigeration 85 (2018) 303–313.

[21] Source for the heatrapy package at GitHub, version v1.0.0, `https://github.com/djsilva99/heatrapy`, 2018.

[22] D. J. Silva, J. S. Amaral, V. S. Amaral, Heatrapy: a flexible python framework for computing dynamic heat transfer processes involving caloric effects in 1.5D systems, SoftwareX 7 (2018) 373–382.

[23] J. H. Lienhard, A Heat Transfer Textbook, Phlogiston press, 4th edn., 2017.

[24] T. Petersen, K. Engelbrecht, C. Bahl, B. Elmegaard, N. Pryds, A. Smith, Comparison between a 1D and a 2D numerical model of an active magnetic regenerative refrigerator, Journal of Physics D: Applied Physics 41 (10) (2008) 105002.

[25] D. J. Silva, B. D. Bordalo, A. M. Pereira, J. Ventura, J. P. Araújo, Solid state magnetic refrigerator, Appl. Energy 93 (2012) 570.

[26] D. J. Silva, J. Ventura, J. P. Araújo, A. M. Pereira, Maximizing the temperature span of a solid state active magnetic regenerative refrigerator, Appl. Energy 113 (2014) 1149.

[27] D. J. Silva, B. D. Bordalo, J. Puga, A. M. Pereira, J. Ventura, J. C. R. E. Oliveira, J. P. Araújo, Optimization of the physical properties of magnetocaloric materials for solid state magnetic refrigeration, Appl. Therm. Eng. 99 (2016) 514.

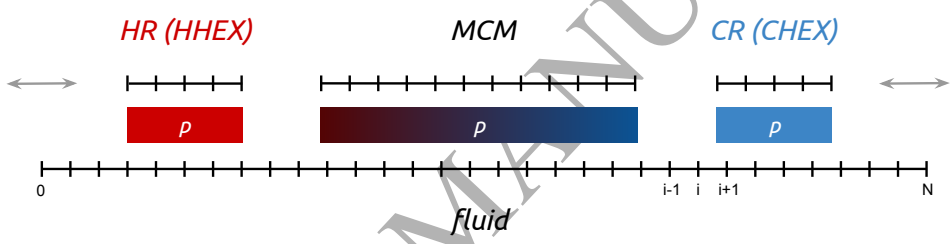

Figure 1: Geometry for the unidimensional active magnetic refrigerator model. The fluid is static, while the MCM, hot and cold reservoirs (HR and CR, respectively) moves cyclically in the horizontal direction. Heat is transferred between the fluid the the 3 remaining elements (p).

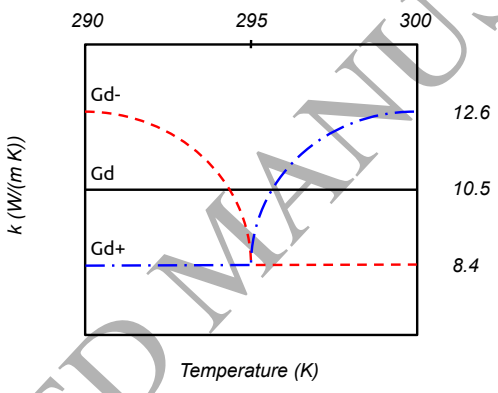

Figure 2: Temperature dependence of the thermal conductivity for three model materials: Gd with fixed k (**Gd**), Gd with increasing k (**Gd+**), and Gd with decreasing k (**Gd-**).

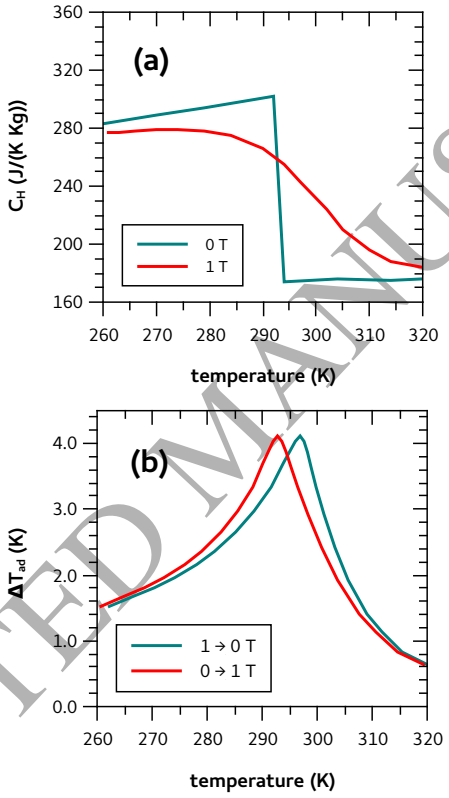

Figure 3: Used temperature dependent **(a)** specific heat at constant magnetic field, **(b)** adiabatic temperature change.

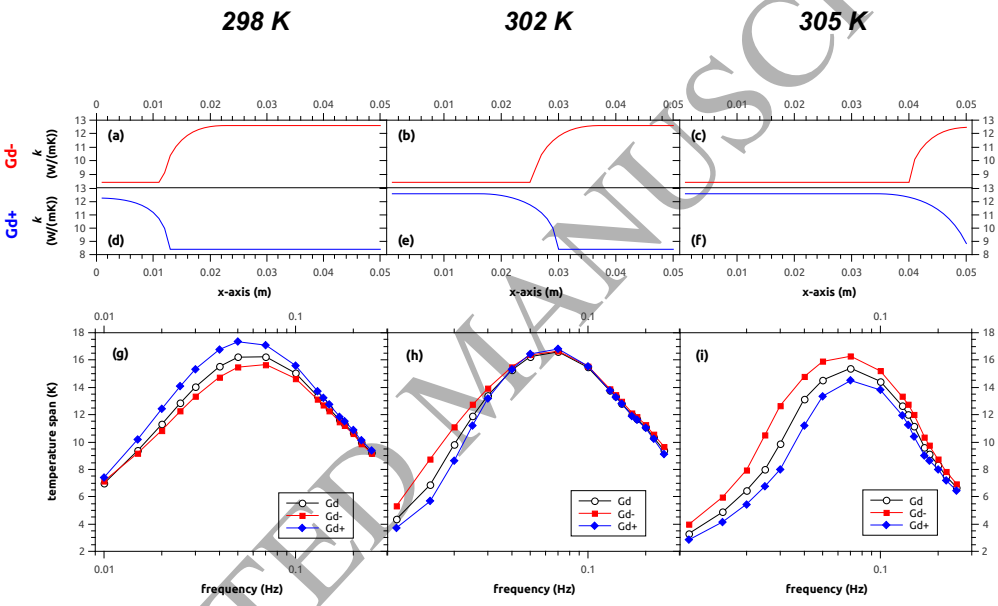

Figure 4: Thermal conductivity along the x-axis of the MCM at the stationary state for Gd- at **(a)** 298 K, **(b)** 302 K and **(c)** 305 K, and for Gd+ at **(d)** 298 K, **(e)** 302 K and **(f)** 305 K. Temperature span as a function of frequency of the 3 MCM model types for the operating temperatures **(g)** 298 K, **(h)** 302 K and **(i)** 305 K.

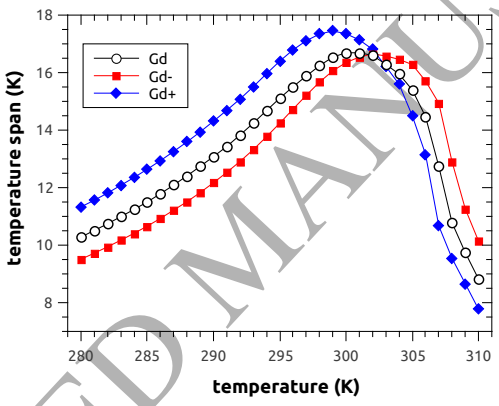

Figure 5: Temperature span of the modeled system as a function of operating temperature for the three MCM model types. The system operates at 0.07 Hz.

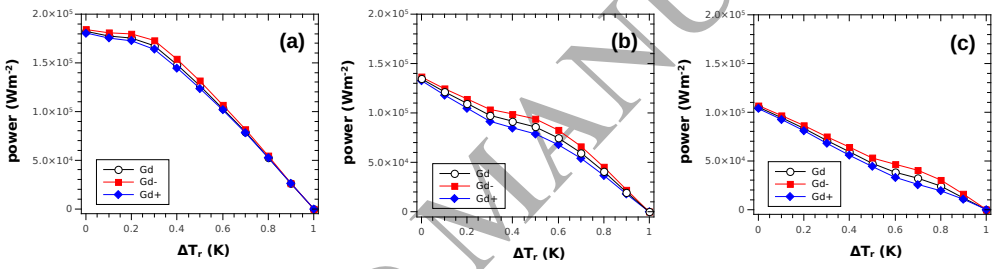

Figure 6: Cooling power per area as a function of temperature span / maximum temperature span ratio (ΔT_r) for the three MCM model types and for the operating temperatures: **(a)** 298 K, **(b)** 302 K and **(c)** 305 K